# Tolerance to rotation of toric monofocal and bifocal intraocular lenses. A theoretical study.

**Authors:** Antonio J. Del Águila-Carrasco, MSc, Alberto Domínguez-Vicent, PhD, Daniel Monsálvez-Romín, MSc, José Juan Esteve-Taboada, PhD, and Eleni Papadatou, PhD

**Affiliation**: Department of Optics, and Optometry, and Vision Sciences. University of Valencia. Spain.

**Disclosure**: The authors report no conflicts of interest and have no proprietary interest in any of the materials mentioned in this article.

**Corresponding author:**

Antonio J. Del Águila-Carrasco

Department of Optics and Optometry and Vision Sciences – University of Valencia

C/ Dr Moliner, 50 – 46100 – Burjassot. Spain.

Telf. +34 963544764. E-mail: antonio.aguila@uv.es

**Abstract**

This manuscript aims to evaluate the tolerance to rotation of a toric monofocal and a toric bifocal intraocular lenses with different cylinder powers. Theoretical designs based on wavefront aberrations were created to simulate a toric monofocal and a toric bifocal intraocular lens. Cylinder power ranged from -1 D to -6 D, in steps of -1 D. Tolerance to rotation was estimated by the visual Strehl ratio based on the optical transfer function (VSOTF) metric. Tolerance to rotation for both monofocal and bifocal intraocular lenses decreased when the cylinder power increased. For the bifocal design studied, the tolerance to rotation was larger for the near focus than for the far, however the overall quality was poorer for the near focus. Our findings show evidence that rotation tolerance depends both on the design of the intraocular lens and the cylinder power. This approach could be useful for predicting the tolerance to rotation of monofocal and multifocal toric intraocular lenses prior the surgery.

**Keywords**: tolerance to rotation; toric intraocular lenses; bifocality; aberrations; visual optics.

## Introduction

Presbyopia is the result of the accommodative ability loss experienced by the aging eye as deterioration of the near vision clarity [1,2]. This loss of accommodation is inherent to the senescence of the human eye and is related to biochemical changes of the crystalline lens structure due to aging [3]. Among various solutions, multifocal corrections are a popular approach for compensating presbyopic symptoms [2]. Many multifocal solutions work under the strategy of simultaneous vision [4], which is based on the projection of several images on the retina at the same time. Depending on the working distance, one of these images will be focused, while the rest will present different amounts of blur. The success of simultaneous vision lies then in the subjects' ability to select the best focused image and suppress the rest [2,4].

Several types of multifocal solutions based on simultaneous vision can be distinguished, according to the symmetry and the structure of the correcting element. Thus, there are symmetrical, asymmetrical, concentric and aspheric designs. The majority of the commercially available solutions in contact lenses (CLs) and some intraocular lenses (IOLs) have concentric designs, which consist of several annular refractive zones for achieving vision at different distances [2]. All these solutions for presbyopia aim to compensate also for the rest of the subjects' refractive errors. Astigmatism is a fairly common refractive error among the population [5,6] and can have a severe impact in visual quality if not corrected. For this purpose, toric multifocal CLs and IOLs are available in the market which aim to increase spectacle independence by correcting astigmatism along with presbyopia, myopia and hyperopia.

The axis of a toric optical solution has to be aligned with the astigmatism axis to correctly compensate the refractive error and, hence, provide good vision. Toric CLs have stabilization systems [7] for avoiding undesired rotations that occur with blinks and can influence the visual performance [8]. When treating with IOLs, however, this issue gets more complex. It is known that IOLs can rotate after they have been implanted in the eye [9–11], which is not impactful for vision if the IOL has rotational symmetry. Nevertheless, if the IOL does not present rotational symmetry, visual outcomes can change depending on the angle of rotation [12,13]. If the IOL is toric, then, even relatively small rotations can have a large impact in the subjects' vision [14,15]. Stability is a crucial factor regarding the efficacy of toric IOLs, since a 10° rotation can reduce the effectiveness of the toric correction by 33%, whereas a rotation of more than 30° can induce undesired astigmatism [16]. Unfortunately, the impact of IOL rotations in visual acuity is evaluated after the IOL has been implanted in the eye, which can lead unavoidably to a follow-up surgery.

Multifocal refractive designs have been previously used to study the impact of the number of zones [17,18] or the zone distribution [17] on vision. In this work, we used these type of simulated typical multifocal corrections based on wavefront aberrations for assessing theoretically the tolerance to rotation of a concentric bifocal and of a monofocal IOL under different cylinder powers when combined with corneal aberrations from different eyes.

## Methods

### Corneal aberrations

Retrospective corneal aberrations from six right eyes of six healthy subjects (26.2 ± 6.1 years old) obtained with the Pentacam HR (Oculus, Wetzlar, Germany) were used in this study. Data comprised Zernike coefficients from the whole cornea up to and including 6th order. Participants gave written informed consent and the study adhered to the tenets of the Declaration of Helsinki. A seventh set of corneal aberrations was introduced into the study. This set is identical to the first, but we substituted the 4th order spherical aberration (SA) value by 0.41 microns (0.20 microns for a 5-mm pupil), which is the typical value for a 60 year-old subject, according to Navarro et al. model cornea [19].

### Intraocular lenses designs

Two IOLs designs were generated for this study: one monofocal and one bifocal. The designs were created using wavefronts [17] as if they were obtained in the pupil plane of the eye and they were made trying to match some characteristics of commercially available lenses. The only aberrations that they presented were astigmatism (since we were interested in toric IOLs) and SA. Both designs were given a Zernike 4th order SA value of -0.24 microns, for a 6-mm pupil, which is a typical value that some commercially available IOLs incorporate [20,21]. Different values of cylinder power were given to the IOLs, depending on the corneal astigmatism we wished to compensate, as it will be explained later.

The bifocal lens was of center-near [2] design and consisted of two different refractive annular concentric zones: a 2-mm diameter central zone

dedicated for near vision with an addition power of 3 D and an annular zone dedicated for far vision.

General procedure

An example of the general methodology followed in this work is illustrated in Figure 1. The IOL's cylinder power in this example is -3 D at 90°. For compensating all the corneal astigmatism with this IOL, the corneal astigmatism should have the same magnitude, but opposite sign. Hence, the astigmatism that we wanted to compensate with the IOL was simulated in the cornea. The axis of the corneal astigmatism was calculated taking into account Zernike coefficients up to 6th order, and the different cylinder powers were simulated in this axis. It should be taken into account that when we refer to the IOL's cylinder throughout this text, we mean the astigmatic power needed to compensate the corneal astigmatism.

Once the astigmatism was set in both the cornea and the IOL, we started rotating the IOL by rotating its wavefront [22]. Rotations from -24° to +24° in steps of 0.5° were simulated for the monofocal IOL, whereas for the bifocal the rotations were simulated from -20° to +20°, using the same step. We considered negative angles as counter-clockwise rotations and positive angles as clockwise rotations. At each rotation angle, a visual Strehl ratio based on the optical transfer function (VSOTF) through-focus curve was computed at a vergence ranging from -2 to +2 D for the monofocal IOL, and from -4 to +1 D for the bifocal IOL. The through-focus step was 0.125 D. The selection of the VSOTF [23,24] is justified by the fact that is an optical quality metric highly correlated with visual acuity [25,26] (VA). Following this, we located the maximum (monofocal IOL) or maxima (bifocal IOL) from the through-focus

curves, which will be called from now on peak VSOTF, and we evaluated the variation of the peak VSOTF with the rotation angle. For assessing the tolerance to rotation, we selected a threshold value that has been used before (VSOTF = 0.12) [17]. This threshold corresponds to a 0.2 logMAR VA [25] and it can be considered as the limit where half of the people show difficulty reading [27]. Therefore, the interval or range of the peak VSOTF curve which was above that threshold indicated the tolerance to rotation of each IOL design.

The tolerance to rotation was assessed for the combination between each IOL design and each of the seven corneal wavefronts and the case where the cornea had zero higher-order aberrations (HOAs). Cylinder power ranging from -1 to -6 D, in -1 D steps, was studied. The negative sign was selected because the lenses prescription is normally given in such way. For the bifocal IOL case, tolerance of rotation was calculated for the far and near vision. Styles-Crawford apodization effect was taken into account in the simulations by defining a Gaussian amplitude transmission pupil [28]. A 4.5-mm pupil was used for all the calculations, since it has been reported as a typical pupil size for presbyopic subjects under photopic conditions [29]. All the calculations were performed using monochromatic light (550 nm).

For exploring the effect of different type of HOAs on the tolerance to rotation of our IOLs designs, a stepwise forward regression [30] was performed. This method performs a multilinear regression and keeps the statistically significant variables within the model, while the non-significant variables are rejected sequentially and do not appear in the final linear model. Therefore, that analysis allowed us to elucidate which aberrations had a significant impact on the tolerance to rotation of the IOLs. For this purpose, the HOAs were grouped

as follows: coma-like aberrations (third and fifth order), trefoil-like aberrations (third and fifth order), spherical-like aberrations (fourth and sixth orders) and astigmatism-like aberrations (fourth and six orders). The root mean square (RMS) error was calculated for each group of aberrations for a 4.5-pupil diameter.

Finally, for illustrating the effect of rotation in image quality, retinal images were simulated by convolving a United States Air Force (USAF) target with the Point Spread Functions (PSFs) of both IOLs designs.

## Results

Table 1 shows the RMS values of the different corneal HOAs of each set considered in this study.

Figure 2 shows the tolerance to rotation of the monofocal IOL (top row) and its tolerance to rotation when corneal aberrations from subject 1 were added to the IOL's wavefront (bottom row). A cylinder of -3 D was selected as an example for this figure. In the left column, the through-focus VSOTF curves are represented for both cases at different rotation angles, whereas the right column shows the variation of the peak VSOTF with the angle of rotation for the different cylinder powers. The horizontal dashed lines indicate the VSOTF threshold (0.12). The peak VSOTF represented in the right panel corresponds to the respective maximum in the through-focus (left panels), which in these cases were zero diopters. Each colour indicates a different cylinder power.

The variation in the tolerance to rotation interval, which corresponds with respect to the sum of the tolerance to rotation in both orientations, with respect to the cylinder power of the monofocal toric IOL can be seen in the top panel of Figure 3. It is clear that the angle interval (considering both orientations), where a monofocal toric IOL can be rotated without too much detriment on the vision, decreases greatly as the cylinder power increases. The bottom panel in Figure 3 shows the individual tolerance to rotation of all the corneal aberration sets under study, the mean value of the seven sets, and the case where the cornea does not present HOAs. From the figure, we can observe that the differences among subjects are generally small. Here, we can see also how the tolerance to rotation decreases with the cylinder power for every corneal aberrations set (different colours).

Figure 4, shows retinal image simulations of how the USAF target is seen through the monofocal toric IOL plus a cornea without HOAs, considering several rotations and three different cylinder powers. It is evident that as the power of the cylinder increases the images get blurrier with smaller rotations.

Similarly to Figure 2, the upper panel of Figure 5 shows the tolerance to rotation of the bifocal IOL design with and without the HOAs of the corneal aberrations set 1. The bottom panel of the figure shows the variations of the peak VSOTF with respect to the angle of rotation for both the far and near foci. As in Figure 2, the angle of rotation and the cylinder power affect the quality of the through-focus curves. The effect of corneal HOAs is more evident in the bifocal case than in the monofocal case.

Figure 6 gives the same information as Figure 3, but for the bifocal toric IOL, for both the far (left column) and the near focus (right column). Again, cylinder power rapidly diminishes the interval of tolerance to rotation. In this case it is worthy to point out the fact that the near focus presented a greater tolerance to rotation than the far focus. However, the far focus showed slightly more inter-individual variability. This could be explained by the fact that the IOL had a center-near design, thus aberrations probably affect more in the peripheral zone which was dedicated to far vision.

Figure 7 shows simulated images of the USAF target that can be seen through the bifocal toric IOL at different angles of rotation and cylinder powers. The group of images at the top corresponds to the far focus, whereas the images at the bottom to the near focus. The quality of the images deteriorated as both the amounts of rotation and cylinder power increased. In the near focus, ghost images corresponding to the far focus can be observed.

Table 2 shows the results of the stepwise linear regression that was performed for exploring which HOAs had a greater influence on the tolerance to rotation of both IOLs designs. According to these results, it seems that the trefoil-like terms have the greater effect on the tolerance to rotation for monofocal toric IOLs, and also for the far focus in the bifocal toric IOL, along with the coma-like terms. Regarding the near focus, the results are more irregular. At low cylinder, the term affecting most the tolerance to rotation is the astigmatism-like; for mid cylinder powers, the aberration terms affecting more the tolerance to rotation are the coma-like terms. Finally, for high cylinder powers, none of the terms yielded any significant interaction.

## Discussion

Rotations of IOLs after implantation can and do occur frequently [9–11]. The magnitude of rotation depends on the IOLs design [31] (haptics, plate, etc.), their adhesive properties [32,33] and the postoperative axial movement of the lens due to capsular bag shrinkage [31]. Rotations can occur soon after the surgery but can also appear in a later stage, around three months afterwards [10]. The magnitude of rotations goes from mild angle values (< 10 degrees) to severe ones (< 30 degrees). Consequently, IOLs' rotations can have a very marked impact on the subjects' visual performance which can lead into IOL's extraction.

Our results showed that in the case of the monofocal IOL the tolerance to rotation barely depends on the subjects' corneal aberrations (see Figure 3). When the cylinder power is high (6 D), the optimal rotation angle is the one we calculated for each subject, whereas for lower cylinder powers, some subjects showed slightly different optimal angles. Aside from this slight difference in the best angle in a few subjects, the inter-individual tolerance to rotation among individuals is similar. This tolerance decreases with cylinder power in a rapid way, which is logical, since the greater the power of the cylinder, the greater the resultant residual astigmatism. A fact worthy of pointing out is that the ideal case (cornea without HOAs) does not yield the highest tolerance results, according to Figure 3. On the contrary, it seems to be in the middle among all the data. Hence, particular sets of corneal HOAs seem to have the ability of increasing slightly the tolerance of rotation of monofocal toric IOLs. This shares the same explanation as the theoretical depth of focus (DoF). Subjects with particular levels of aberrations (generally SA) show an increase in DoF, but a

decrease in optical quality[35,36], since there is a trade-off between those two parameters.

Regarding the bifocal design, we performed the analysis of the two main foci, corresponding to the nominal power (far focus) and the addition power (near focus), separately. In the representation of the peak VSOTF with respect to the angle of rotation (Figure 5), we can see that the optical quality of the near focus is worse than the one of the far focus. This is due to the fact that we wanted to simulate a typical bifocal IOL, in which the distribution of energy is inclined towards the area dedicated for far correction. Despite the quality being worse, the tolerance to rotation was better for the near vision than for the far. This could be explained by the selection of a center-near design, due to the fact that the residual astigmatism could have a larger impact in the peripheral zone than in the central one.

For both foci, the variation of the tolerance to rotation with regards to the cylinder power is similar to that of the monofocal IOL. It can be noticed from Figure 6 that for the near vision, the ideal case (IOL plus cornea without HOAs) yielded the highest tolerance to rotation among all the corneal aberrations sets plus bifocal IOL configurations. Regarding the far vision, the addition of some corneal HOAs improved slightly the tolerance of rotation.

Comparing to the monofocal, in the bifocal case there seemed to exist more inter-individual variability and more asymmetries within the tolerance to rotation, mostly for the far focus. This may be due to the fact that the bifocal IOL had a more complex design than the monofocal IOL. It is also worthy to outline that the tolerance to rotation of the monofocal IOL exceeded the one of the bifocal IOL for both of its foci. This reinforces the importance that rotations

experienced by multifocal IOLs can have in the subjects' visual performance. This impact can be even greater in more complex designs, such as trifocal IOLs [36,37] or extended-range IOLs [38,39].

The corneal aberrations used in this work were measured to young people who do not need IOL implantation in normal conditions. Nevertheless, several studies showed that corneal aberrations are very subject dependant [40], with the SA being the main contributor to age-related changes in HOAs [41,42]. For this reason, we added an extra corneal aberrations set, having a SA of 0.41 µm for a 6-mm pupil that corresponds to a 60-years old model cornea [19]. The addition of this SA value practically did not change the outcomes regarding tolerance to rotation. Its greatest impact was found in the peak VSOTF, which was lower due to having a higher value of SA.

Special consideration has to be taken with the interpretation of the tolerance to rotation values. These values could vary slightly if we had used another optical quality metric to calculate the through-focus curves. The use of the VSOTF is justified by the high correlation found between this metric and VA [25], however, that does not mean that other metrics could not have been used. Another important aspect is the selection of the threshold for acceptable vision. We chose 0.2 logMAR VA [26], which corresponds to a value of 0.12 for VSOTF, as explained in the Methods section. This is an absolute threshold, nevertheless, there is the possibility of selecting a relative one, as has been done in many studies about DoF [43,44]. The problem with the relative threshold, as Yi et al. [45] showed, is that in order to correlate the theoretical DoF with the subjective one, it was better to assume that each subject could have his/her own threshold value.

From the results, it can be assumed that there are some particular corneal HOAs that could improve slightly the tolerance to rotations in toric IOLs (Table 2). Generally, as the corneal HOAs increased, the tolerance to rotation seemed to decrease. Nevertheless, in some cases, for small amounts of corneal HOAs (mostly trefoil and coma-like terms), there existed an improvement in tolerance to rotation. Our results could indicate that depending on the design of the toric IOL and on the cylinder power, the tolerance to rotation could be improved with the addition of certain aberrations to the IOL, always at the expense of a possible decrease in optical quality caused by these aberrations.

Although this theoretical approach can be a useful tool for predicting the tolerance to rotation of different IOLs, it has several limitations that need to be taken into account. The first one being that the IOLs created in this work were theoretical and the only aberrations present on them were SA and astigmatism. Nevertheless, the design used here for the bifocal is similar to the one presented by some commercially available bifocal corrections [46] and the amount of SA selected is a typical one. Also, rotationally symmetrical IOLs have normally negligible amount of non-rotational aberrations [47]. Another limitation is that the simulations in this study were all done under the assumption of monochromatic light (550 nm), thus removing the possible effect of chromatic aberration upon the tolerance to rotation.

In summary, this method could be a powerful tool to predict the tolerance to rotation of monofocal and multiple zones multifocal toric IOLs before the implantation of the actual lens occurs. In addition, a more personalized prediction can be made according to the subjects' corneal aberrations, since

they can be combined with different IOLs designs. Another application of this method goes in the direction of the toric IOL optimization and design. Several parameters can be tested (area of the different zones, number of zones, other aberrations, etc.) to try to find an IOL that presents a high tolerance to rotation. Finally, this method can show the impact of rotations in different toric IOL designs when combined with corneal aberrations in the retinal image quality, which could be an approximation of how the patient actually sees with a rotated toric IOL.

**Funding**

This work was supported by the University of Valencia, Spain [Atracció de Talent Research Fellows UV-INV-PREDOC14-179135 and UV-INV-PREDOC13-110412]; the Ministerio de Educación, Cultura y Deporte, Spain [FPU13/05332]; and the European Commission [Ageye FP7-PEOPLE-2013-ITN-608049].

## References


[1] A. Duane, An attempt to determine the normal range of accommodation at various ages, being a revision of Donder's experiments., Trans. Am. Ophthalmol. Soc. 11 (1908) 634–41.

[2] W.N. Charman, Developments in the correction of presbyopia I: spectacle and contact lenses., Ophthalmic Physiol. Opt. 34 (2014) 8–29.

[3] A. Glasser, M.C. Campbell, Presbyopia and the optical changes in the human crystalline lens with age., Vision Res. 38 (1998) 209–29.

[4] W.N. Charman, Developments in the correction of presbyopia II: surgical approaches., Ophthalmic Physiol. Opt. 34 (2014) 397–426.

[5] T. Ferrer-Blasco, R. Montés-Micó, S.C. Peixoto-de-Matos, J.M. González-Méijome, A. Cerviño, Prevalence of corneal astigmatism before cataract surgery., J. Cataract Refract. Surg. 35 (2009) 70–5.

[6] J. Katz, J.M. Tielsch, A. Sommer, Prevalence and risk factors for refractive errors in an adult inner city population., Invest. Ophthalmol. Vis. Sci. 38 (1997) 334–40.

[7] T.B. Edrington, A literature review: the impact of rotational stabilization methods on toric soft contact lens performance., Cont. Lens Anterior Eye. 34 (2011) 104–10.

[8] A. Tomlinson, W.H. Ridder, R. Watanabe, Blink-induced variations in visual performance with toric soft contact lenses., Optom. Vis. Sci. 71 (1994) 545–9.

[9] E.F. Marques, T.B. Ferreira, P. Simões, Visual Performance and Rotational Stability of a Multifocal Toric Intraocular Lens, J. Refract. Surg. 32 (2016) 444–450.

[10] C.K. Patel, S. Ormonde, P.H. Rosen, A.J. Bron, Postoperative intraocular lens rotation: a randomized comparison of plate and loop haptic implants., Ophthalmology. 106 (1999) 2190–5; discussion 2196.

[11] M.J. Saldanha, L. Benjamin, C.K. Patel, Postoperative rotation of a 3-piece loop-haptic acrylic intraocular lens, J. Cataract Refract. Surg. 35 (2009) 1751–1755.

[12] S. Bonaque-González, S. Ríos, A. Amigó, N. López-Gil, Influence on Visual Quality of Intraoperative Orientation of Asymmetric Intraocular Lenses., J. Refract. Surg. 31 (2015) 651–7.

[13] A. Felipe, J.M. Artigas, A. Díez-Ajenjo, C. García-Domene, C. Peris, Modulation transfer function of a toric intraocular lens: evaluation of the changes produced by rotation and tilt., J. Refract. Surg. 28 (2012) 335–40.

[14] E.E. Pazo, O. Richoz, R. McNeely, Z.A. Millar, T.C.B. Moore, J.E. Moore, Optimized Visual Outcome After Asymmetrical Multifocal IOL Rotation., J. Refract. Surg. 32 (2016) 494–6.

[15] A. Felipe, J.M. Artigas, A. Díez-Ajenjo, C. García-Domene, P. Alcocer, Residual astigmatism produced by toric intraocular lens rotation, J. Cataract Refract. Surg. 37 (2011) 1895–1901.

[16] K. Shimizu, A. Misawa, Y. Suzuki, Toric intraocular lenses: correcting astigmatism while controlling axis shift., J. Cataract Refract. Surg. 20 (1994) 523–6.

[17] P. de Gracia, C. Dorronsoro, S. Marcos, Multiple zone multifocal phase designs, Opt. Lett. 38 (2013) 3526.

[18] R. Legras, D. Rio, Effect of Number of Zones on Subjective Vision in Concentric Bifocal Optics., Optom. Vis. Sci. 92 (2015) 1056–62.

[19] R. Navarro, J.J. Rozema, M.-J. Tassignon, Optical Changes of the Human Cornea as a Function of Age, Optom. Vis. Sci. 90 (2013) 587–598.

[20] A. Alarcon, C. Canovas, R. Rosen, H. Weeber, L. Tsai, K. Hileman, P. Piers, Preclinical metrics to predict through-focus visual acuity for pseudophakic patients., Biomed. Opt. Express. 7 (2016) 1877–88.

[21] L. Wang, D.D. Koch, Custom optimization of intraocular lens asphericity, J. Cataract Refract. Surg. 33 (2007) 1713–1720.

[22] L. Lundström, P. Unsbo, Transformation of Zernike coefficients: scaled, translated, and rotated wavefronts with circular and elliptical pupils., J. Opt. Soc. Am. A. Opt. Image Sci. Vis. 24 (2007) 569–77.

[23] L.N. Thibos, X. Hong, A. Bradley, R.A. Applegate, Accuracy and precision of objective refraction from wavefront aberrations, J. Vis. 4 (2004) 9.

[24] D.R. Iskander, Computational aspects of the visual Strehl ratio., Optom. Vis. Sci. 83 (2006) 57–9.

[25] J.D. Marsack, L.N. Thibos, R.A. Applegate, Metrics of optical quality derived from wave aberrations predict visual performance., J. Vis. 4 (2004) 322–8.

[26] X. Cheng, A. Bradley, L.N. Thibos, Predicting subjective judgment of best focus with objective image quality metrics., J. Vis. 4 (2004) 310–21.

[27] S.K. West, G.S. Rubin, A.T. Broman, B. Muñoz, K. Bandeen-Roche, K. Turano, How does visual impairment affect performance on tasks of everyday life? The SEE Project. Salisbury Eye Evaluation., Arch. Ophthalmol. (Chicago, Ill. 1960). 120 (2002) 774–80.

[28] R.A. Applegate, V. Lakshminarayanan, Parametric representation of Stiles-Crawford functions: normal variation of peak location and directionality., J. Opt. Soc. Am. A. 10 (1993) 1611–23.

[29] N. Chateau, J. De Brabander, F. Bouchard, H. Molenaar, Infrared pupillometry in presbyopes fitted with soft contact lenses., Optom. Vis. Sci. 73 (1996) 733–41.

[30] M.A. Efroymson, Multiple Regression Analysis, in: A. Ralston, H.S. Wilf (Eds.), Math. Methods Digit. Comput., John Wiley, New York, 1960.

[31] V. Petternel, R. Menapace, O. Findl, B. Kiss, M. Wirtitsch, G. Rainer, W. Drexler, Effect of optic edge design and haptic angulation on postoperative intraocular lens position change., J. Cataract Refract. Surg. 30 (2004) 52–7.

[32] R.J. Linnola, L. Werner, S.K. Pandey, M. Escobar-Gomez, S.L. Znoiko, D.J. Apple, Adhesion of fibronectin, vitronectin, laminin, and collagen type IV to intraocular lens materials in pseudophakic human autopsy eyes. Part 1: histological sections., J. Cataract Refract. Surg. 26 (2000) 1792–806.

[33] M. Lombardo, G. Carbone, G. Lombardo, M.P. De Santo, R. Barberi, Analysis of intraocular lens surface adhesiveness by atomic force microscopy., J. Cataract Refract. Surg. 35 (2009) 1266–72.

[34] Y. Benard, N. Lopez-Gil, R. Legras, Optimizing the subjective depth-of-focus with combinations of fourth- and sixth-order spherical aberration., Vision Res. 51 (2011) 2471–7.

[35] R. Legras, Y. Benard, N. Lopez-Gil, Effect of coma and spherical aberration on depth-of-focus measured using adaptive optics and computationally blurred images., J. Cataract Refract. Surg. 38 (2012) 458–69.

[36] F.T.A. Kretz, D. Breyer, K. Klabe, P. Hagen, H. Kaymak, M.J. Koss, M. Gerl, M. Mueller, R.H. Gerl, G.U. Auffarth, Clinical Outcomes After Implantation of a Trifocal Toric Intraocular Lens, J. Refract. Surg. 31 (2015) 504–510.

[37] P. Mojzis, K. Majerova, A.B. Plaza-Puche, L. Hrckova, J.L. Alio, Visual outcomes of a new toric trifocal diffractive intraocular lens, J. Cataract Refract. Surg. 41 (2015) 2695–2706.

[38] B. Cochener, Concerto Study Group, Clinical outcomes of a new extended range of vision intraocular lens: International Multicenter Concerto Study., J. Cataract Refract. Surg. 42 (2016) 1268–1275.

[39] J.J. Esteve-Taboada, A. Domínguez-Vicent, A.J. Del Águila-Carrasco, T. Ferrer-Blasco, R. Montés-Micó, Effect of Large Apertures on the Optical Quality of Three Multifocal Lenses., J. Refract. Surg. 31 (2015) 666–76.

[40] S. Amano, Y. Amano, S. Yamagami, T. Miyai, K. Miyata, T. Samejima, T. Oshika, Age-related changes in corneal and ocular higher-order wavefront aberrations, Am. J. Ophthalmol. 137 (2004) 988–992.

[41] P. Artal, E. Berrio, A. Guirao, P. Piers, Contribution of the cornea and internal surfaces to the change of ocular aberrations with age., J. Opt. Soc. Am. A. Opt. Image Sci. Vis. 19 (2002) 137–43.

[42] T. Oshika, S.D. Klyce, R.A. Applegate, H.C. Howland, Changes in corneal wavefront aberrations with aging., Invest. Ophthalmol. Vis. Sci. 40 (1999) 1351–5.

[43] R. Xu, A. Bradley, N. López Gil, L.N. Thibos, Modelling the effects of secondary spherical aberration on refractive error, image quality and depth of focus., Ophthalmic Physiol. Opt. 35 (2015) 28–38.

[44] S. Marcos, E. Moreno, R. Navarro, The depth-of-field of the human eye from objective and subjective measurements., Vision Res. 39 (1999) 2039–49.

[45] F. Yi, D.R. Iskander, M.J. Collins, Estimation of the depth of focus from wavefront measurements., J. Vis. 10 (2010) 3.1-9.

[46] S. Plainis, D.A. Atchison, W.N. Charman, Power profiles of multifocal contact lenses and their interpretation., Optom. Vis. Sci. 90 (2013) 1066–77.

[47] D.H. Chang, K.M. Rocha, Intraocular lens optics and aberrations, Curr. Opin. Ophthalmol. 27 (2016) 298–303.

## Figure legends

**Fig. 1** Illustration of the methodology followed in this work. The black dashed lines indicate the cylinder axis of the IOL. The top part of the figure shows the wavefront of a theoretical toric monofocal IOL (no HOAs) when added to the wavefront of an astigmatic cornea (no HOAs), resulting into a perfect compensation of the corneal astigmatism (1.a). Residual corneal astigmatism was apparent when the IOL was rotated 15° clockwise (1.b). Bottom part of the figure shows the same, but with a center-near bifocal concentric IOL.

**Fig. 2** Top left panel shows several monofocal IOL through-focus VSOTF curves at different angles of rotation (solid curve indicates perfect centration; dashed line corresponds to a rotation of 4°; and dotted line shows a 10° rotation). Top right panel shows the maximum of the through-focus in the left (peak VSOTF) with respect to the angle of rotation. Different colours indicate different cylinder powers. Bottom row shows the same, but when HOAs from subject 1 cornea were added to the calculations. The horizontal dashed lines indicate the VSOTF threshold (0.12). All the graphs correspond to a toric IOL with -3 D of cylinder.

**Fig. 3** Variation of the tolerance to rotation interval (sum of the tolerance to rotation in both orientations) of the monofocal toric IOL regarding the cylinder power (top panel). Symbols are different for each corneal set. The open circle corresponds to the monofocal IOL without the presence of HOAs. Black line represents the mean values of the seven sets without including the case where there was only the IOL. The bottom panel shows the individual tolerance to rotation for three values of cylinder (1, 3 and 6 D). The marker indicates the angle where the quality (peak VSOTF) was optimum, whereas the bars

represent the tolerance to rotation (VSOTF ≥ 0.12) to both orientations. Negative angle values are counter clockwise rotation; positive values are clockwise rotations.

**Fig. 4** USAF targets obtained with the monofocal IOL at different amounts of rotation (columns) and for different cylinder powers (rows). Only one orientation is represented here, since the IOL plus cornea without HOAs does not have any asymmetrical aberration, both orientations are the same.

**Fig. 5** Through-focus VSOTF curves for the bifocal IOL plus cornea without HOAs (top left panel) and for the IOL with the corneal HOAs of set 1 (top right panel). Variation of the peak VSOTF with respect to the angle of rotation for the far focus of the IOL plus cornea without HOAs (mid left panel), and for the IOL plus corneal aberrations from set 1 (mid right panel). Bottom row shows same as before but for the near focus. The horizontal dashed lines indicate the VSOTF threshold (0.12). Symbols and colours are the same as in Figure 2. All the graphs correspond to a toric IOL with -3 D of cylinder. Note that the scale of the y axis changes throughout the panels.

**Fig. 6** Top row shows the variation experienced by the tolerance to rotation with respect to the cylinder power for all the corneal aberrations and for the IOL plus cornea without HOAs, for both the far (left) and near foci (right). The bottom row shows the individual tolerance to rotation, alongside the mean of the seven corneal aberrations sets, and the IOL plus cornea without HOAs case. The left column shows the results for the far focus whereas the right for the near focus. Symbols and colours are those described in Figure 3.

**Fig. 7** USAF targets images of the bifocal toric IOL at different angles of rotation (columns), and cylinder powers (rows). The upper stack of images corresponds

to the far focus (a), whereas the bottom stack (b) shows the images obtained for the near focus. Only one orientation is represented here, since the IOL plus cornea without HOAs does not have any asymmetrical aberration, both orientations are the same.

Figure 1

Click here to download high resolution image

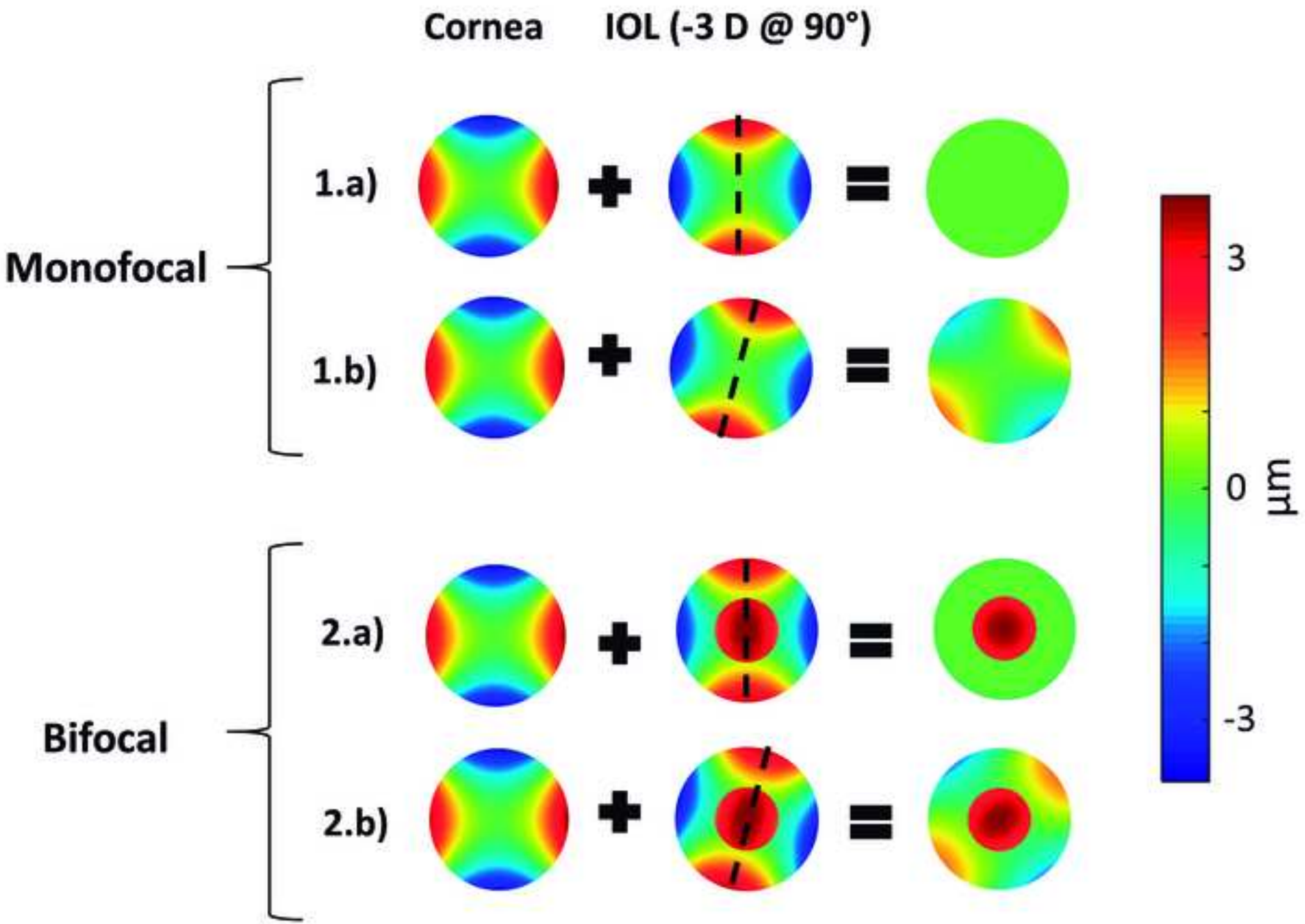

**Figure 2**

Click here to download high resolution image

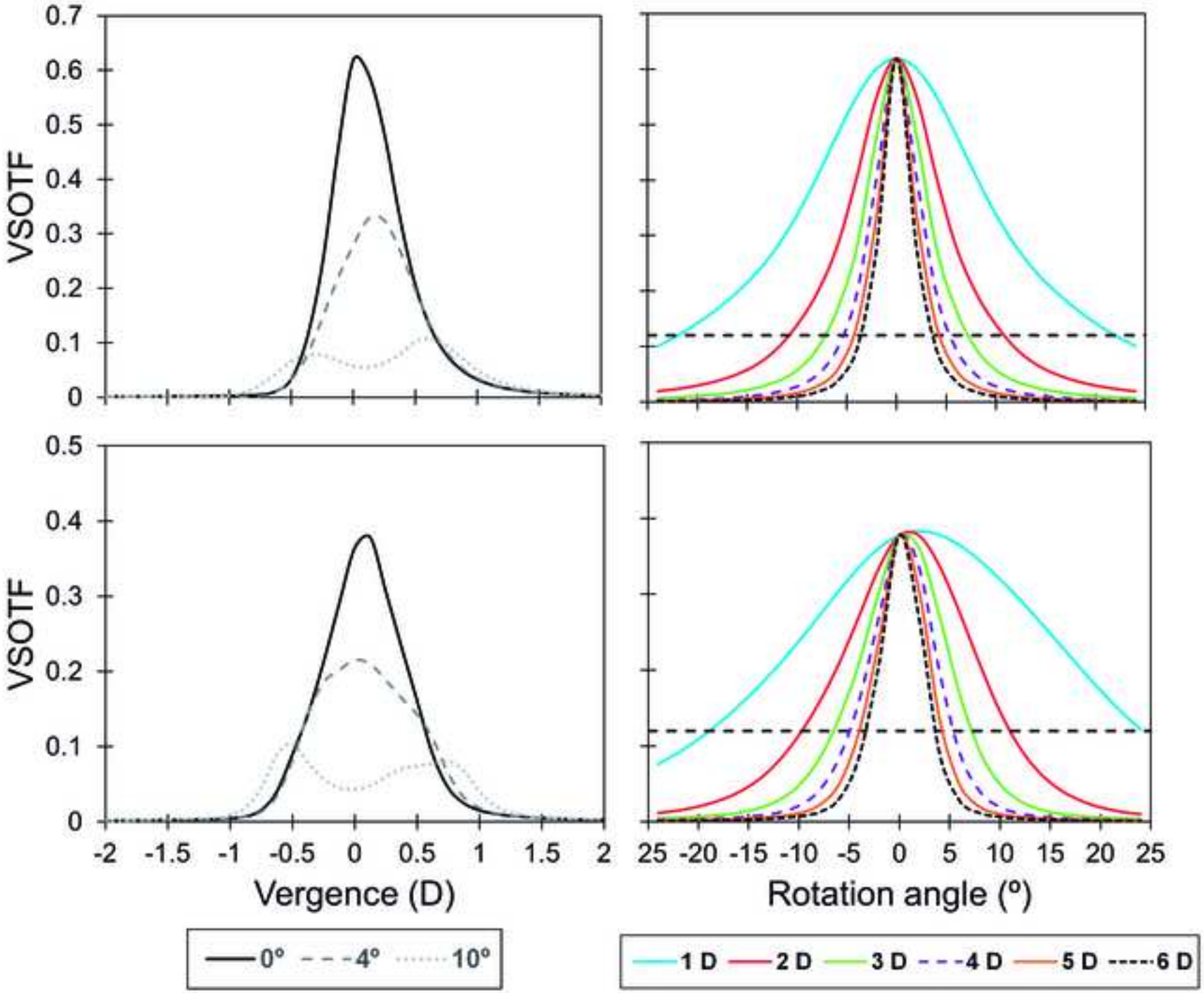

**Figure 3**

**Click here to download high resolution image**

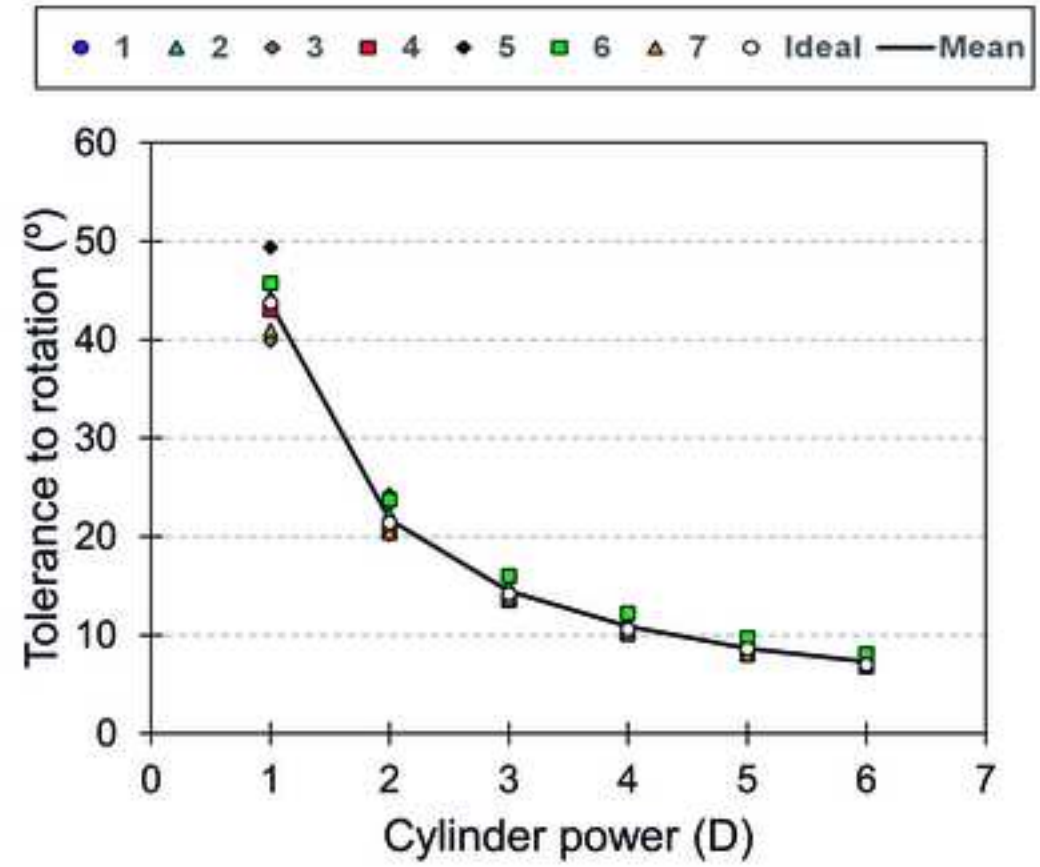


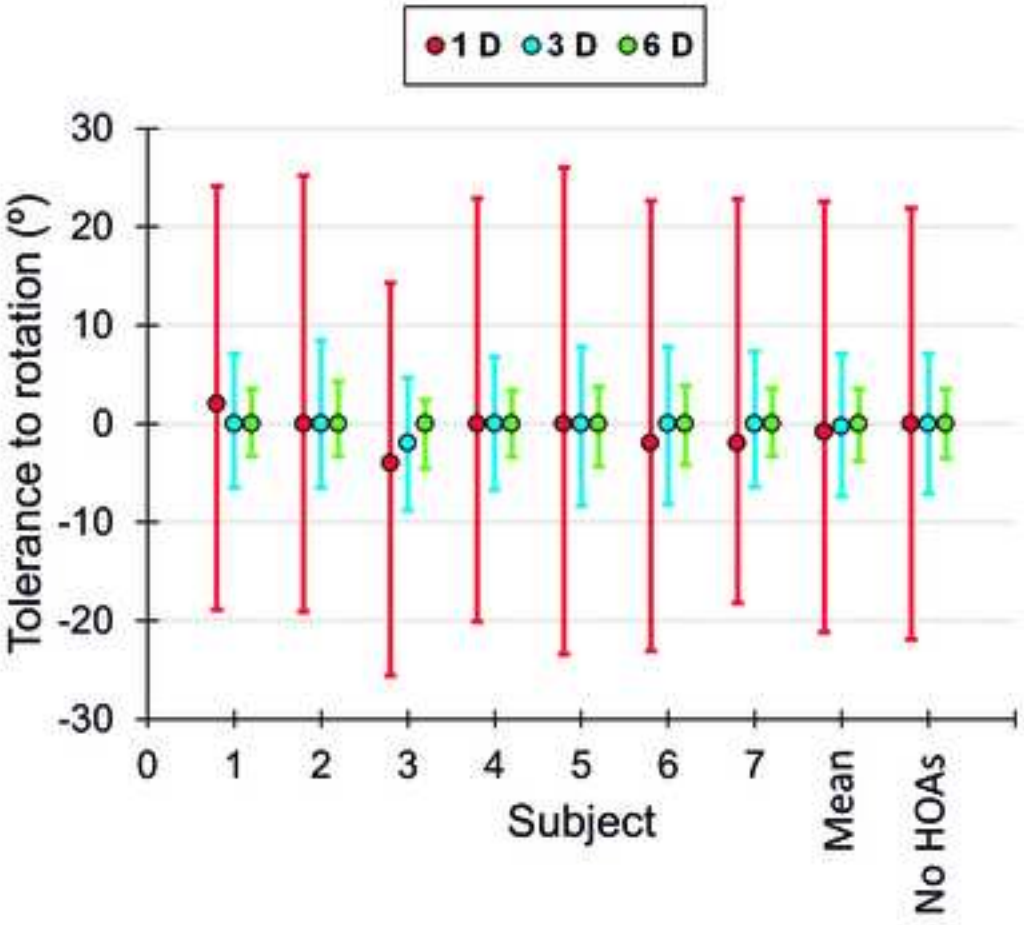

Figure 4

Click here to download high resolution image

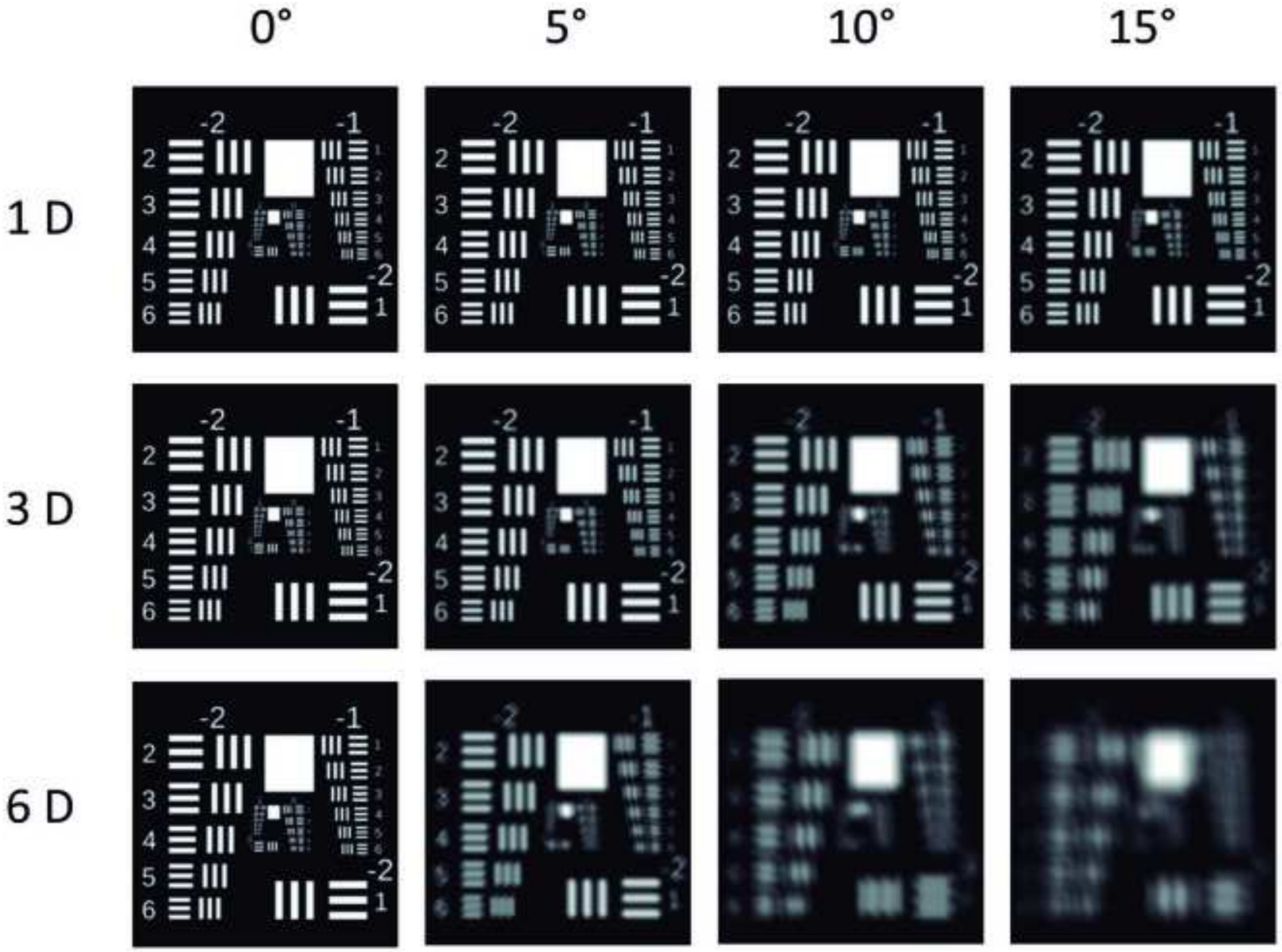

Figure 5

Click here to download high resolution image

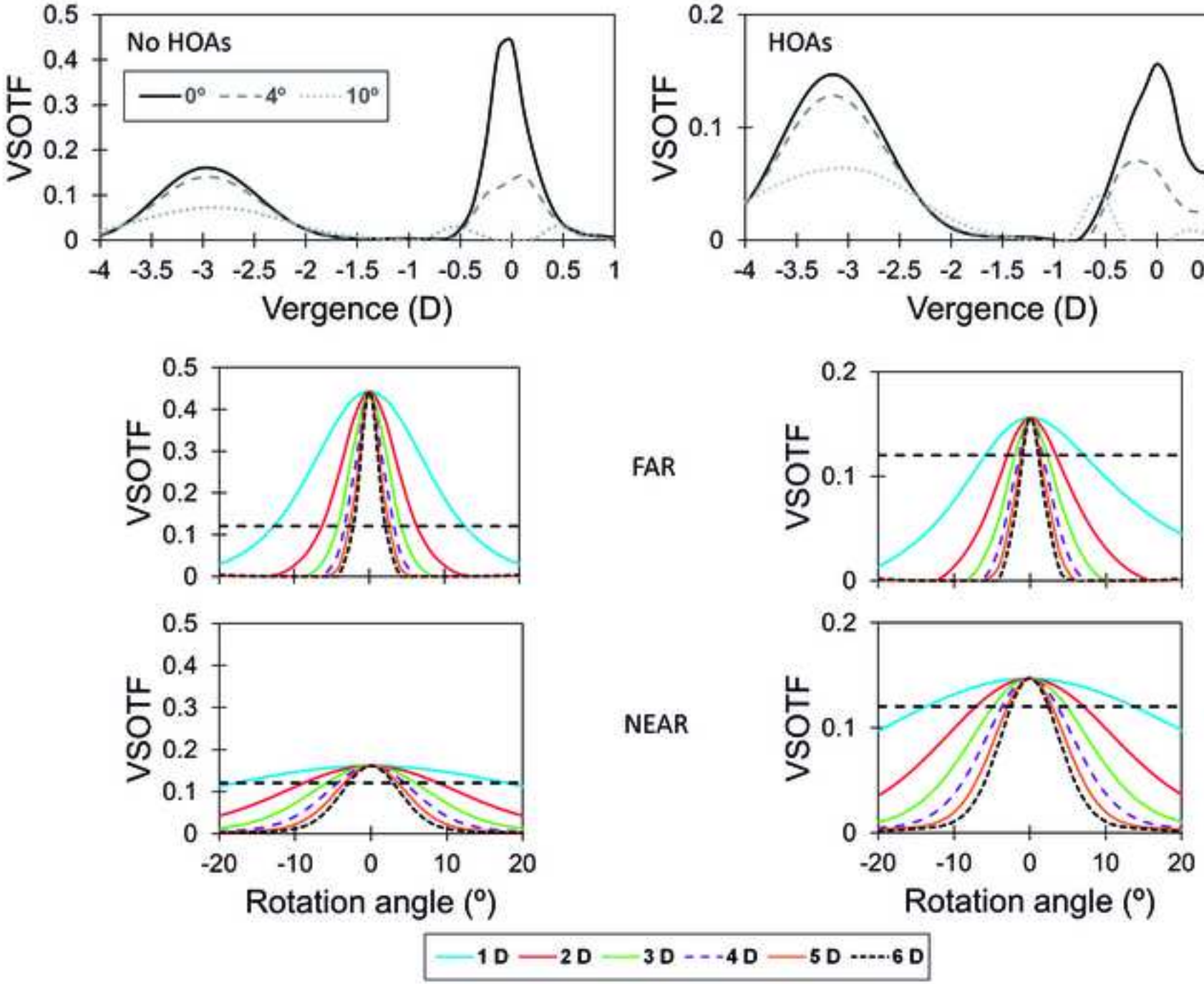

Figure 6

Click here to download high resolution image

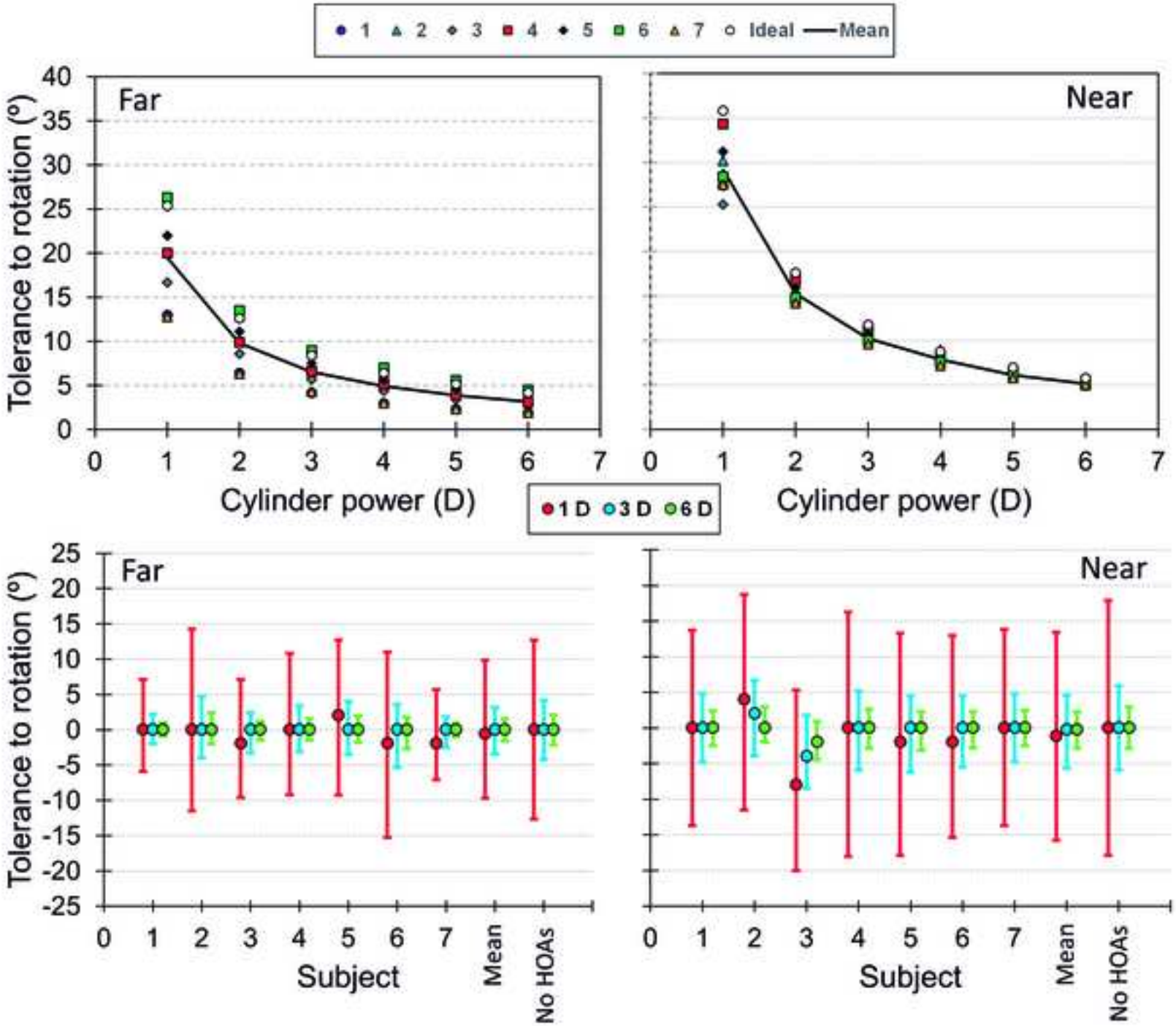

**Figure 7**

Click here to download high resolution image

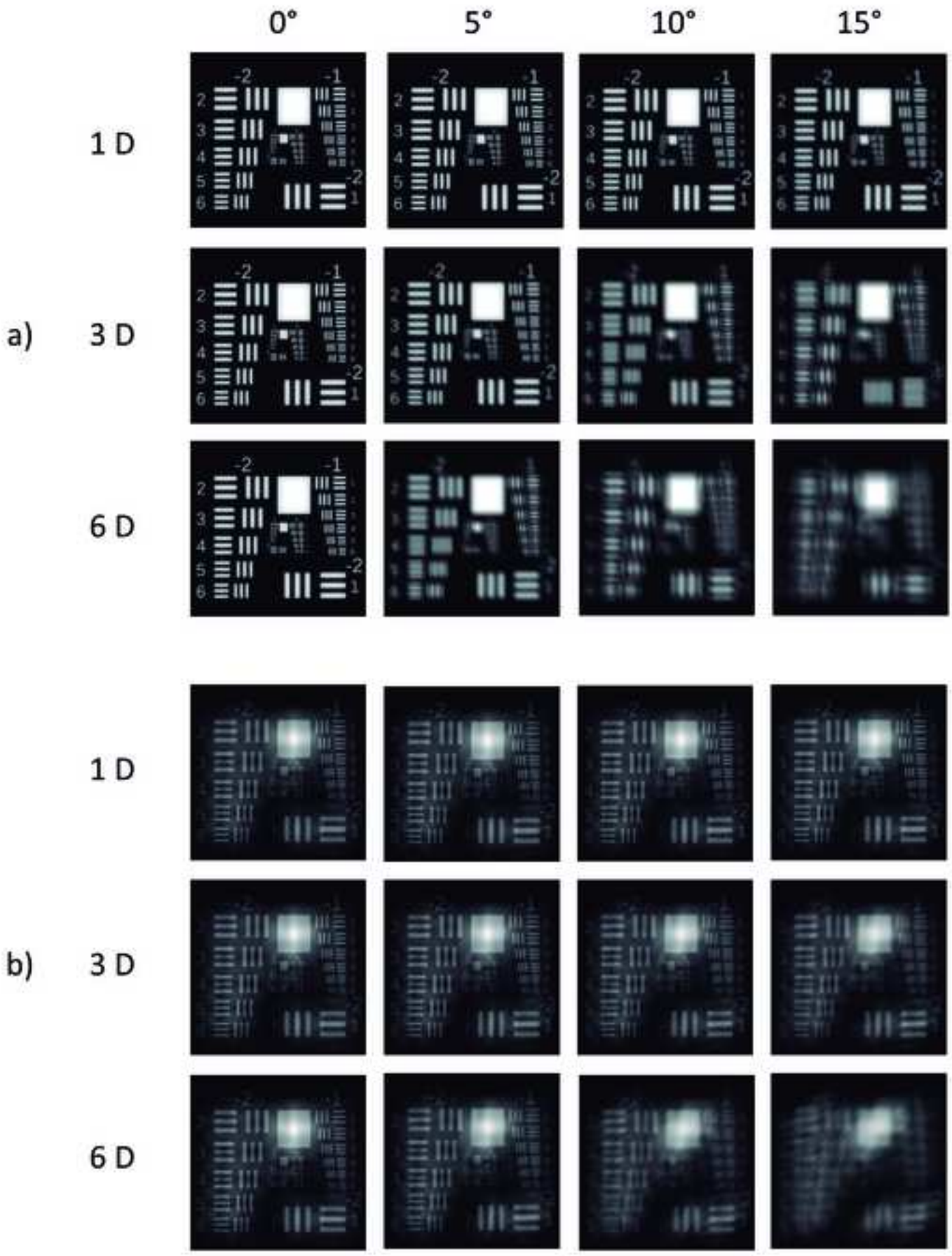

**Table 1.** Different corneal HOAs RMS expressed in microns for every subject. The last row is subject's 1 corneal aberrations set, with a fourth-order spherical aberration of 0.41 for a 6-mm pupil. All the RMS were calculated for a 4.5-mm pupil.

| Subject | Coma-like | Trefoil-like | Spherical-like | Astigmatism-like | Tetrafoil-like | HOAs |
|---|---|---|---|---|---|---|
| 1 | 0.1005 | 0.1307 | 0.0537 | 0.0362 | 0.0327 | 0.1811 |
| 2 | 0.0615 | 0.0381 | 0.0386 | 0.0389 | 0.0149 | 0.0922 |
| 3 | 0.0813 | 0.0928 | 0.0599 | 0.0584 | 0.0326 | 0.1529 |
| 4 | 0.0496 | 0.1182 | 0.0557 | 0.0074 | 0.0109 | 0.1405 |
| 5 | 0.0616 | 0.0496 | 0.0385 | 0.0262 | 0.0680 | 0.1150 |
| 6 | 0.0513 | 0.0555 | 0.0606 | 0.0340 | 0.0267 | 0.1065 |
| 7 | 0.1005 | 0.1307 | 0.1140 | 0.0362 | 0.0327 | 0.2071 |

**Table 2.** Results yielded by the stepwise linear regression for each cylinder power and for both IOLs designs simulated in this study. In each cell, the significant term/s is/are shown, along with the respective *p*-value. A dash indicates that none of the terms was significant in order to explain the tolerance to rotation.

| | Monofocal IOL | Bifocal IOL | |
|---|---|---|---|
| Cylinder (D) | | Far | Near |
| 1 | - | Trefoil-like ($p$ = 0.007) and coma-like ($p$ = 0.021) | Astigmatism-like ($p$ = 0.004) |
| 2 | Trefoil-like ($p$ = 0.021) | Trefoil-like ($p$ = 0.006) and coma-like ($p$ = 0.021) | Coma-like ($p$ = 0.043) |
| 3 | Trefoil-like ($p$ = 0.016) | Trefoil-like ($p$ = 0.005) and coma-like ($p$ = 0.021) | Coma-like ($p$ = 0.036) |
| 4 | Trefoil-like ($p$ = 0.015) | Trefoil-like ($p$ = 0.006) and coma-like ($p$ = 0.014) | - |
| 5 | Trefoil-like ($p$ = 0.011) | Trefoil-like ($p$ = 0.005) and coma-like ($p$ = 0.016) | - |
| 6 | Trefoil-like ($p$ = 0.010) | Trefoil-like ($p$ = 0.001) and astigmatism-like ($p$ = 0.013) | - |